Int. J. Exp. Path. (2010), 91, 288–301
doi: 10.1111/j.1365-2613.2010.00713.x

ORIGINAL ARTICLE

Variation in characteristics of islets of Langerhans in insulin-resistant, diabetic and non-diabetic-rat strains

Huw Bowen Jones, David Nugent and Richard Jenkins
Pathology Department, Global Safety Assessment, AstraZeneca Pharmaceuticals, Alderley Park, Macclesfield, Cheshire, UK

INTERNATIONAL JOURNAL OF EXPERIMENTAL PATHOLOGY

Summary

Assessment of the histopathological and plasma biochemical characteristics of diabetic and non-diabetic rat strains [Han and AP Wistar, lean and obese Zucker Fatty (ZF), and lean and obese Zucker Diabetic Fatty (ZDF) rats] was performed at 6 or 14 weeks of age. Wistar and lean ZF and ZDF rats showed no or minimal islet pathology or plasma biochemical alterations at both timepoints. Obese ZFs were euglycaemic at both timepoints and mildly and severely hyperinsulinaemic at 6 and 14 weeks respectively. Islet morphology was normal at 6 weeks but at 14 weeks, islet hyperplasia was present with a minority showing degenerative changes namely, β-cell vacuolation, vascular congestion and haemorrhage with minimal mononuclear cell and T lymphocytic infiltration. Obese ZDFs were euglycaemic and moderately hyperinsulinaemic at 6 weeks and severely hyperglycaemic with minor hypoinsulinaemia at 14 weeks. Obese ZDFs at 6 weeks showed mainly normal islets with some displaying degeneration (ranging from β-cell vacuolation alone to the features described above). At 14 weeks, islet degeneration was more severe and widespread: β-cell death was present in numerous islets at low level. Islet β-cell numbers were reduced or absent (with associated reduction in insulin immunostaining) within the islets that now consisted predominantly of fibroblasts, collagen and mononuclear cells. Fibroproliferation consisting of smooth muscle actin-α-positive tissue was associated with mononuclear cell infiltration. Some fibrous scars were visible indicative of lost islets. Islet degeneration in obese ZF and ZDF rats was not accompanied by a reduction in β-cell proliferation or in compensatory proliferation of β-cell neogenic clusters. In the light of recent reports of adaptive and inflammation-mediated degenerative changes in human non-insulin dependent diabetes mellitus (NIDDM) islets, the hypertrophy/hyperplasia of β-cells and islet degeneration involving infiltration by monocyte/macrophages in obese ZF and obese ZDF rats respectively offers substantial potential for elucidation of the processes involved.

Keywords
biochemistry, diabetes, Han Wistar rat, insulin resistance, islets of Langerhans, pathology, Wistar rat, Zucker Diabetic Fatty Rat, Zucker Fatty rat

Received for publication: 18 June 2009
Accepted for publication: 26 January 2010

Correspondence:
Huw Bowen Jones
Pathology Department
Global Safety Assessment
AstraZeneca Pharmaceuticals
Alderley Park
Macclesfield
Cheshire SK10 4TG
UK
Tel.: 044 (0) 1625 514552
Fax: 044 (0) 1625 514812
E-mail: huw.jones@astrazeneca.com

The incidence of obesity-associated, non-insulin dependent diabetes mellitus (NIDDM) has become a modern health issue of global importance (Shimabukuro *et al.* 1998). Numerous adverse influences, mainly of hyperglycaemia and hyperlipidaemia have been recognised to affect β-cell metabolic pathways and islet functional integrity both directly and indirectly (Stefan *et al.* 1982; Clark *et al.* 1988; Zhou *et al.* 2000; Listenberger *et al.* 2003; Poitout & Robertson 2008). The key to understanding the nature of this important human disease has been assessment of functional and morphological alterations of islets and their causes, but few studies on non-diabetics and diabetics have been performed due to issues of tissue availability and rapid pancreatic deterioration post mortem. As a consequence, literature reports have been affected by generally low patient numbers, variable gender distribution, duration and severity of disease and variation in treatment regimes (Stefan *et al.* 1982; Rahier *et al.* 1983; Kloppel *et al.* 1985). Kloppel *et al.* (1985) reported that in NIDDM, β-cells are always present, irrespective of the severity and duration of the disease indicative of a secretory defect rather than functionally deficient β-cell mass. Furthermore, in autopsy samples from obese, insulin resistant, hyperinsulinaemic individuals, substantially increased β-cell mass (60%), indicative of prediabetic functional adaptation is evident. Following the development of NIDDM, not only are islet number and total β-cell volume reduced significantly, but other islet endocrine cell cohorts are also similarly diminished. The characteristic features of islet morphology in insulin resistance and overt diabetes are islet hypertrophy/hyperplasia and degeneration respectively.

In large part, due to the relative inaccessibility of human pancreatic tissue acquisition, the focus of investigations on this disease has been in animals and has intensified significantly since the recognition and development of a number of rodent models of NIDDM that permit access to and investigation of the cellular and molecular processes involved. The obese Zucker Fatty (ZF) and obese Zucker Diabetic Fatty (ZDF) rat strains are characterised by a leptin receptor mutation that renders leptin signal detection ineffective leading to hyperphagia, hyperleptinaemia, insulin resistance, diabetes and obesity (Clark *et al.* 1983). Obese ZFs and obese ZDFs are euglycaemic at 5–6 weeks but obese ZDFs become increasingly hyperglycaemic and hypoinsulinaemic, develop diabetes at about 10 weeks with progressive islet failure, eventually dying at 30+ weeks of age due to diabetes-related issues (Clark *et al.* 1983; Tokuyama *et al.* 1995; Janssen *et al.* 1999).

Our primary focus has been on understanding changes in islets of Langerhans of non-diabetic animals (namely Han and AP Wistar, lean ZF and lean ZDF rats) during islet adaptation and eventual failure in those strains (namely obese ZF and obese ZDF rats) that undergo age-related loss of glucose homeostasis due to insulin resistance and diabetes. The characterisation of the degree of variation between islets of Langerhans of individual animals and the rat strains assessed was important to our investigation due to parallel in vitro assessments on isolated islets, and was done using histopathological, immunohistochemical and plasma biochemical approaches. In this regard, acquisition of an understanding of inter-strain variation in intra- and inter-animal islet characteristics was an important goal.

Materials and methods

Animals and husbandry

Four strains of rats were used in this study namely, AP Wistar (Alderley Park, AstraZeneca Pharmaceuticals, Macclesfield, UK), Han-Wistar (Charles River, Margate, Kent, UK), lean and obese ZFs (Alderley Park colony) and lean and obese ZDFs (Charles River Laboratories, Indianapolis, IN, USA). The lean ZFs and lean ZDF rats were homozygous and heterozygous respectively, based on in-house genotyping. All animals were male, were maintained on sawdust in smooth bottomed plastic cages, permitted free access to standard diet (SDS modified R&M No 1, Special Diet Services, Witham, Essex, UK) and potable drinking water in a climate-controlled room (maintained at 20 °C, 12 h dark/light cycle with approximately 70% relative humidity). Five rats of a single strain were housed in each cage and entered the study at 5 weeks of age to allow a 1 week acclimatisation period. All animals were used in the fed state with no fasting period employed. Ten animals of each strain were used and maintained until they were either 6 or 14 weeks old: at each time, five were terminated by terminal narcosis via CO_2/O_2 inhalation and a heart-puncture blood sample taken into EDTA. Pancreas was removed and fixed by immersion in 10% neutral buffered formalin for 24–48 h before standard processing and embedding in paraffin wax. The pancreas was embedded to demonstrate the head/tail orientation and to maximise the area of tissue sections (3–4 μm thick), which were stained with haematoxylin and eosin and examined by light microscopy for subsequent histopathological examination.

Immunohistochemistry

Histochemical demonstration of fibrous tissue was performed using Masson's Trichrome stain (Pearse 1985).

Insulin immunohistochemistry was used to identify β cells, assess their density (percent β cells/islet area) and

distribution in islets, location and characteristics of β cell neogenic clusters. Insulin combined with Ki67 immunohistochemistry was used for determination of β cell replicative rate. Mononuclear cell infiltrates were stained with an anti-ED1 antibody (110 kDa single chain glycoprotein present in the outer membrane of monocyte/macrophage lysosomes, CD68 homologous) in order to identify these cells and distinguish them from other inflammatory cells and fibroblasts that were present in the same tissues. Possible lymphocytic presence in these infiltrates was determined by CD3 and CD79a immunohistochemistry for T- and B-lymphocytes respectively. Immunostaining for smooth muscle actin-α (SMA-α) was performed in order to assess altered islet vascularisation and the identity of cells involved in islet mesenchymal proliferation/fibrosis.

For all immunohistochemical techniques, pancreatic sections were dewaxed in xylene and rehydrated through graded alcohols to water. When necessary, antigen retrieval was performed by microwave at 110 °C for 2 min in EDTA buffer at pH 8 using the Milestone RHS2 microwave (Milestone RHS-2, Sorisole, Italy) with pressure vessel followed by washing of sections in water before being placed onto a Labvision Immunostainer (Thermo Fisher Scientific, Runcorn, UK) where the remainder of the immunohistochemical staining was performed. Sections were first washed in Tris buffered saline with 0.05% Tween (TBST) followed by blockade of endogenous peroxidase with 3% hydrogen peroxide in TBST for 10 min. Another TBST wash preceded incubation of sections for 20 min with a 1:20 normal serum block in TBST or Dako Protein Block (X0909; Dako Denmark A/S, Glostrup, Denmark), followed by application of primary antibody, performed with a technique appropriate for each antibody, followed by another TBST wash and visualized with DAB (or with a combination of DAB and Vector SG for dual labelling) for 10 min. Following a water wash, sections were counterstained in Carazzi's haematoxylin for 1 min washed in water for 5 min and coverslipped. All dilutions were in TBST.

Insulin immunohistochemistry was performed (without antigen retrieval) using a guinea pig anti-insulin primary antibody (Dako, A0564) diluted 1:50, followed by a biotinylated swine anti-goat/mouse/rabbit secondary antibody (Dako, E0453) diluted 1:200 and a strept-ABC/HRP kit (Dako, K0377). Immunostaining for ED1 required high temperature antigen retrieval and was performed using a monoclonal mouse anti-rat ED1 primary antibody (MCA341R; AbD Serotec, Kidlington, UK) diluted 1:200 for 60 min. Immunostaining for SMA-α was performed without antigen retrieval using monoclonal mouse anti SMA-α (A2547; Sigma Aldrich Company Ltd, Gillingham, UK at 1:1000) for 30 min. Both ED1 and αSMA were detected with mouse Envision-HRP kit (Dako, K4007) for 30 min. CD3 and CD79a immunostaining required high temperature antigen retrieval. CD3 was performed using a polyclonal rabbit anti-CD3 (18-0102; Invitrogen Ltd, Paisley, UK) diluted 1:50 for 60 min and detected with rabbit EnVision-HRP (Dako, K4011) for 30 min. CD79a was performed using a monoclonal mouse anti-CD79a (ab3121; Abcam plc, Cambridge, UK) diluted 1:200, followed by a rabbit anti mouse secondary antibody (Dako, Z0456) diluted 1:400 and detected with rabbit EnVision-HRP for 30 min.

For dual IHC labelling of insulin and Ki67, the method for insulin described above was used first, except that Vector SG (SK-4700; Vector Laboratories, Peterborough, UK for 5 min) was substituted for DAB. Prior to application of the reagents for the second antibody, sections were washed in water and microwaved at 110 °C for 2 min (EDTA buffer pH 8.0). After cooling, sections were washed in water, and placed on a Labvision immunostainer, which applied hydrogen peroxide for 10 min, followed by a 5 min wash in TBST and 20 min incubation with Dako Protein Block (Dako, X0909). The protein block was blown off the sections before the monoclonal mouse anti-rat Ki67 antibody (MM1, Vector, VP-K452) diluted 1:50 in TBST was applied for 2 h. Detection of Ki-67 was performed using a mouse peroxidase anti-peroxidase IgG method at 1:50 dilution for 30 min and, after a TBST wash, sections were immersed in Dako DAB kit for 10 min and counterstained with Carazzi's haematoxylin for 1 min.

Omission of the primary IgG on sections of 6 weeks old Han Wistar pancreatic tissues was included as negative control.

Insulin immunopositivity was visualised as brown staining of β cell cytoplasm. In dual-stained preparations of insulin and Ki67, insulin staining was defined by grey Vector SG positive cytoplasm and Ki67 positivity by a DAB-positive (brown) nucleus.

Image analysis

Islets were defined as clusters of seven or more β cells in association with other morphologically identifiable endocrine cells. All data were obtained from sections immunostained either for insulin alone, or, double stained insulin/Ki67.

Islet image capture was performed using a MRc5 camera (Axiocam; Carl Zeiss Ltd, Welwyn Garden City, UK) from a Leica DMRB microscope (×20 objective) and analysed using KS400 3.0 software. Light source intensity and image hue, brightness and saturation were standardised. Islets were identified and images stored. Individual islet perimeters, islet size, total islet cell number, number and area of insulin

positive (β) cells and the percentage of islet insulin staining (IPIA, %) were semi-automatedly determined. All insulin-positive cells in tissue sections were counted, including faintly positive cells seen in 14-week-old ZDF rats. The total number of Ki67- and insulin-positive cells in islets was counted and the cell replication fraction calculated as a percentage of the total number of insulin positive cells.

Aggregates of β cells generated via neogenesis (neogenic clusters) were defined as insulin positive clusters of two to fifteen β cells present in the exocrine pancreas that were not associated with other islet (hormone) cells (Rosenberg 1995) and were assessed by the method of Paris *et al.* (2003). Briefly, the total area of pancreatic sections immunostained for insulin alone was measured using KS400 3.0 software by manual drawing to define islet perimeter and the total number of neogenic clusters counted and expressed as the number per tissue area (N/cm^2) in one section per animal. Student's *t*-test with two tailed distribution was used to calculate the significance of differences between groups.

Plasma biochemistry

Blood (1 ml) was taken into EDTA-coated tubes and separated by centrifugation at 1200–1500 ***g***, 4 °C for 10 min. The plasma fraction was removed into a sample cup for clinical chemistry analysis (approximately 400 µl) and 1.5 ml micro tubes for insulin analysis (100 µl). Plasma levels of glucose, lactate, non-esterified fatty acids (NEFA), triglyceride, cholesterol and fructosamine were assayed by photometric analysis on a Roche P800 Modular analyser (Roche Diagnostics, Burgess Hill, West Sussex, UK) in accordance with the manufacturer's guidelines.

Plasma insulin levels were assessed by enzyme-linked immunosorbent assay (ELISA) using the commercially available Mercodia Ultrasensitive Rat Insulin ELISA kit, (Mercodia AB, Uppsala, Sweden) in accordance with the manufacturer's instructions. Briefly, plates pre-coated with insulin-specific antibodies were incubated with plasma sample prior to detection using a peroxidase-conjugated secondary antibody and substrate to provide a colorimetric endpoint.

Results

Plasma biochemistry

Data for the 6 and 14 weeks samples are presented in Table 1.

Table 1 Plasma biochemistry at 6 and 14 weeks

	6 weeks					
	AP	**HW**	**Lean ZF**	**Obese ZF**	**Lean ZDF**	**Obese ZDF**
Glucose (mM)	9.54 ± 0.79	10.6 ± 0.42	8.54 ± 0.27	10.3 ± 0.76	8.56 ± 0.45	8.18 ± 0.62
Insulin (ng/ml)	1.10 ± 0.20‡	1.24 ± 0.23‡	0.67 ± 0.13‡	2.76 ± 0.48†	0.30 ± 0.03‡	10.6 ± 2.78†‡
Free fatty acids (mM)	0.21 ± 0.04	0.22 ± 0.04	0.13 ± 0.02	0.14 ± 0.04	0.20 ± 0.02	0.20 ± 0.04
Triglycerides (mM)	1.01 ± 0.09‡	1.23 ± 0.15	0.54 ± 0.03‡	1.32 ± 0.04†	0.84 ± 0.08‡	3.06 ± 0.25†‡
Cholesterol (mM)	2.80 ± 0.21	1.84 ± 0.22‡	2.10 ± 0.04‡	3.32 ± 0.15†	2.92 ± 0.11	3.42 ± 0.16†
Fructosamine (µM)	126 ± 3.6‡	125 ± 2.9‡	123 ± 1.5‡	143 ± 2.6†	125 ± 1.6‡	139 ± 2.6†
Lactate (mM)	4.41 ± 0.57	6.13 ± 0.43	3.24 ± 0.49‡	5.22 ± 0.35	3.98 ± 0.42	4.97 ± 0.41
	14 weeks					
	AP	HW	Lean ZF	Obese ZF	Lean ZDF	Obese ZDF
Glucose (mM)	7.86 ± 0.61	9.20 ± 1.04‡	6.62 ± 0.34*	6.48 ± 0.54*	7.94 ± 0.49	32.5 ± 1.6*†‡
Insulin (ng/ml)	3.28 ± 0.42*‡	4.68 ± 1.87‡	2.06 ± 0.34*‡	37.7 ± 11*†	0.70 ± 0.14*‡	2.94 ± 0.2*†‡
Free fatty acids (mM)	0.12 ± 0.03	0.24 ± 0.05	0.13 ± 0.01	0.15 ± 0.02	0.36 ± 0.04*‡	0.46 ± 0.1*‡
Triglycerides(mM)	1.73 ± 0.10*	2.18 ± 0.45	0.71 ± 0.12	1.49 ± 0.68	1.45 ± 0.12*	3.62 ± 0.2‡
Cholesterol (mM)	2.98 ± 0.25*‡	1.76 ± 0.12*‡	1.96 ± 0.10‡	7.80 ± 1.8*†	2.72 ± 0.18‡	4.52 ± 0.3*†‡
Fructosamine (µM)	137 ± 1*	133 ± 5	116 ± 1*	147 ± 2	124 ± 3	258.8 ± 9.1*†‡
Lactate (mM)	4.78 ± 0.39	5.84 ± 0.64	3.33 ± 0.34‡	5.63 ± 0.45†	3.09 ± 0.48‡	3.60 ± 0.5‡

*P value of <0.05 *vs.* 6 weeks equivalent.
†P value of <0.05 *vs.* lean equivalent.
‡P value of <0.05 *vs.* obese ZF.

6 weeks. Minor differences only were present in blood parameters between non-diabetic AP and HW strains. Mean plasma insulin concentration of all rat strains with the exception of obese ZFs and obese ZDFs was within the range of 0.3–1.2 ng/ml. Plasma insulin was raised slightly in obese ZF rats above HW values (2.2×) but was substantially elevated in obese ZDF rats (8.6×). Mean plasma glucose concentration of all rat strains was within the range of 8.2–10.6 mmol/l. Obese ZDF and ZF rats at 6 weeks were euglycaemic with glucose values of 8.2 and 10.4 mmol/l respectively. Lean ZFs and ZDFs displayed significantly lower values of insulin and triglycerides by comparison with all other strains except obese ZDFs, which exhibited 2–3× higher triglycerides than HW. Free fatty acids were within the range 0.13–0.72 nM in all strains, no elevation seen in either obese ZF or, obese ZDF rats. Other values were not notably altered outside the inter-strain range.

14 weeks. Mean plasma insulin concentration of all rat strains, with the exception of obese ZFs was within the range of 0.7–4.7 ng/ml demonstrating a small age-related increase. Obese ZFs showed a group mean hyperinsulinaemia of 32.8 ng/l, whereas the insulin concentration of obese ZDF rats displayed a moderate reduction to 2.9 ng/l at 14 weeks (10.6 ng/l at 6 weeks). Glucose values were unchanged in all strains except in obese ZDFs, which exhibited a 4× increase by comparison with their euglycaemic values at 6 weeks. In general, free fatty acids and triglyceride values showed minor differences by comparison with 6 weeks samples but in both ZDF strains, free fatty acids were significantly elevated above mean values for other groups at this later time. Triglycerides were elevated mildly in obese ZDFs only. Cholesterol was raised in obese ZF and ZDF rats by approximately 4× and 1.6× respectively, by comparison with levels in corresponding lean strains. Plasma fructosamine was raised (2×) in obese ZDF rats by comparison with their 6 weeks old counterparts. The mean plasma triglycerides concentration in obese ZDF rats was 3.6 mmol/l, which represented a significant elevation above that seen in other obese and lean strains at 14 weeks.

Other values were not notably altered outside the inter-strain range of values.

Pathology

AP and Han Wistar rats. Islets of both strains showed no pathology at either 6 or 14 weeks (Figure 1). Typically,

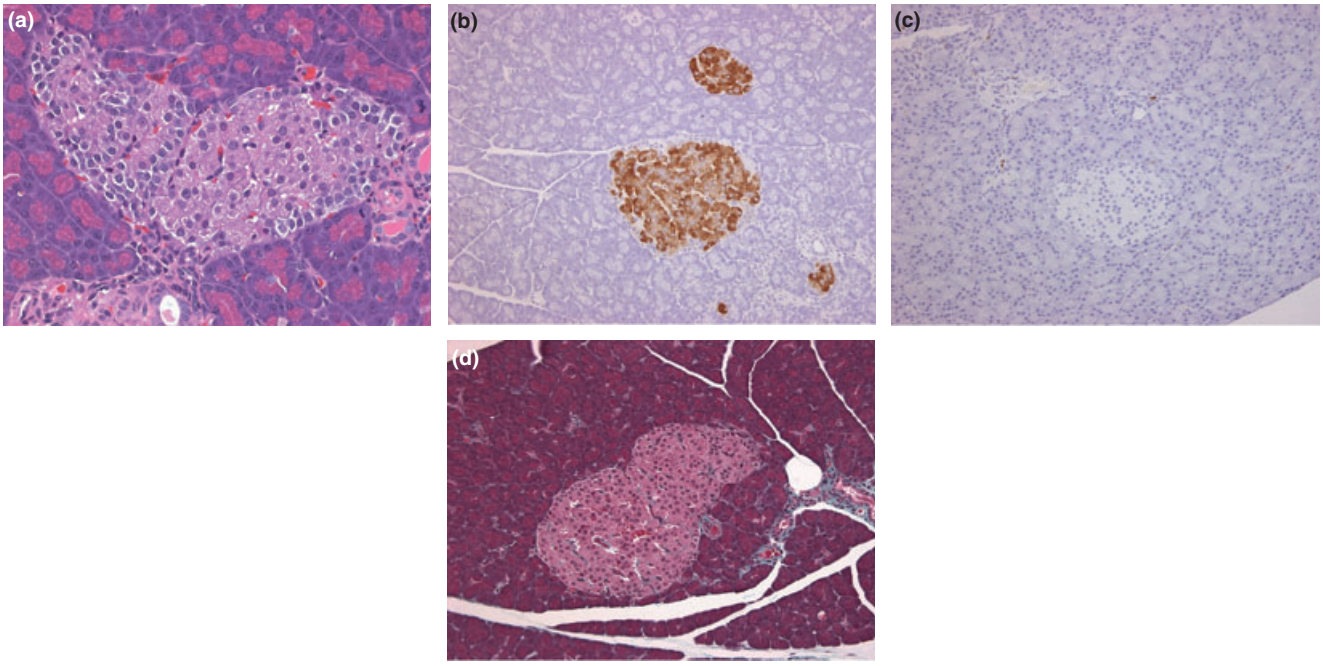

Figure 1 Non-diabetic rat (Han Wistar) islet characteristics. (a) 14 weeks, normal appearance of islet showing a central core of β cells enveloped by a peripheral, largely continuous mantle of non- β cell endocrine cells (H&E), (b) 14 weeks, anti-insulin IHC showing diffuse, homogeneous distribution of insulin in β cells only. Note the presence of small clusters of β cells and the clear differences between the central, β cell core and the peripheral, non-β cell endocrine cells, (c) 14 weeks, macrophage infiltration into islets is almost absent, with few present in peri-ductal and perivascular locations (ED1, IHC), (d) 14 weeks, virtual absence of significant fibrous tissue/collagen in islets and present in peri-vascular locations (Masson's Trichrome).

islets consisted of small, rounded aggregates of mildly eosinophilic cells, the regular periphery of which displayed a more or less continuous, monolayer of small α (glucagon), γ (pancreatic polypeptide) and δ cells (somatostatin) about the central mass of larger β-cells (insulin). The number of β-cells in the majority of small islets was usually less than 30, but in a few larger islets that were occasionally associated with exocrine ducts, their numbers were substantially greater. Islet insulin immunostaining at both times was consistently intense and homogeneous both within and between islets and showed only minor variation between individual β cells. Mononuclear cell/macrophage infiltration (ED1 positive) and fibrous tissue (Masson's Trichrome stain) were minor features and associated always with islet vasculature at both timepoints. SMA-α immunostaining was present consistently in vascular media, pericytes and in periductal myofibroblasts and/or smooth muscle cells at both timepoints. Masson's Trichrome staining demonstrated no differences in distribution or amount of intra-islet fibrous tissue at the times examined. No extravascular T or B lymphocytes were present in islets at any time.

Lean and obese Zucker rats. Lean ZF rats showed no islet pathology at either 6 or 14 weeks. At 6 weeks, obese ZF islets did not show pathological features. However, at 14 weeks, substantial changes were apparent in that both adaptive and degenerative alterations were present together (Figure 2). Commonly, the islet population in individual animals was heterogeneous in that some small islets appeared normal, others were hypertrophic/hyperplastic (adaptation) and displayed irregular outlines whilst a minority, were degenerative. The adaptive changes were either, of a purely hyperplastic/hypertrophic nature with numerous islets being considerably enlarged or, these features were coincident in islets that displayed degenerative features of variable severity. Degenerative changes were characterised by β-cell vacuolation and commonly, recent haemorrhage into islet tissue from quite markedly dilated blood vessels. In the absence of haemosiderin pigmentation, it is possible that haemorrhage was due to post mortem tissue handling with associated mechanical damage to abnormally delicate blood vessels. Additionally, monocyte infiltration into, but most frequently, circumferentially around islets was observed in very few instances within a tissue section and was often associated with numerous large SMA-α-positive cells with prominent fusiform nuclei and few, smaller fibroblasts: this tissue resembling active fibroproliferation. Hypertrophic/hyperplastic islets also showed increased fibrous tissue deposition (Masson Trichrome stain and SMA-α-positive) in association with vascular distribution that displayed a reticular pattern, effectively separating β cells into groups (Figure 2f). The features of individual islet degeneration, its incidence and severity showed considerable intra- and inter-animal variation. A similar, variable multifocal distribution of islet fibrosis of minor severity was focussed in perivascular or periductal locations. It was striking that the majority of islets at this time appeared normal with only a few showing the changes described above.

Insulin immunostaining in lean ZF rats at both ages and obese ZFs at 6 weeks was identical with that seen in AP or Han Wistar animals; all islets, irrespective of size showing intense, homogeneous distribution. However, at 14 weeks, the pattern of insulin staining in obese ZF rats, had changed significantly with neogenic β cell clusters and smaller islets displaying an intense, uniform immunopositivity whilst larger islets (including those showing degenerative features), exhibiting a heterogeneous staining pattern characterised by intense or pale insulin immunostaining of individual β cells. SMA-α immunostaining of lean ZFs at both timepoints and obese ZFs at 6 weeks showed no change as compared with AP or Han Wistars. At 14 weeks, obese ZFs displayed increased, highly variable SMA-α islet tissue immunostaining, which occasionally was very substantial, and was seen in the majority of islets in all animals. The staining defined the fibrous/vascular tracts that separated small aggregates of β cells in the majority of islets as well as the fibrous tissue that was a feature of a minority of islets at this time. In those few islets exhibiting peripheral aggregates of ED1-positive mononuclear cells, the associated tissue was strongly SMA-α-positive. Neither CD3 nor CD79a-positive lymphocytes were present in any islets examined although these were present in adjacent lymph nodes when present, the former also being seen in occasional pancreatitic lesions.

Lean and obese ZDF rats. No pathological changes in islet morphology were evident in lean ZDFs at either 6 or 14 weeks. By comparison with lean ZDFs, obese ZDF animals showed substantial changes in islet morphology at 6 weeks (Figure 3). The majority of islets in all animals were mildly enlarged, showed hypertrophy/hyperplasia, with slightly irregular contours and slight compression of adjacent exocrine tissue. Mononuclear cell infiltration (ED1 immunostaining) was generally minimal and was not associated with diffuse β-cell vacuolation that was present in many islets at this time. However, in a few islets, the degenerative changes observed were much more severe and identical to those described above for obese ZF rats at 14 weeks. Islet vascular congestion with some recent haemorrhage was a striking feature of numerous islets in these animals.

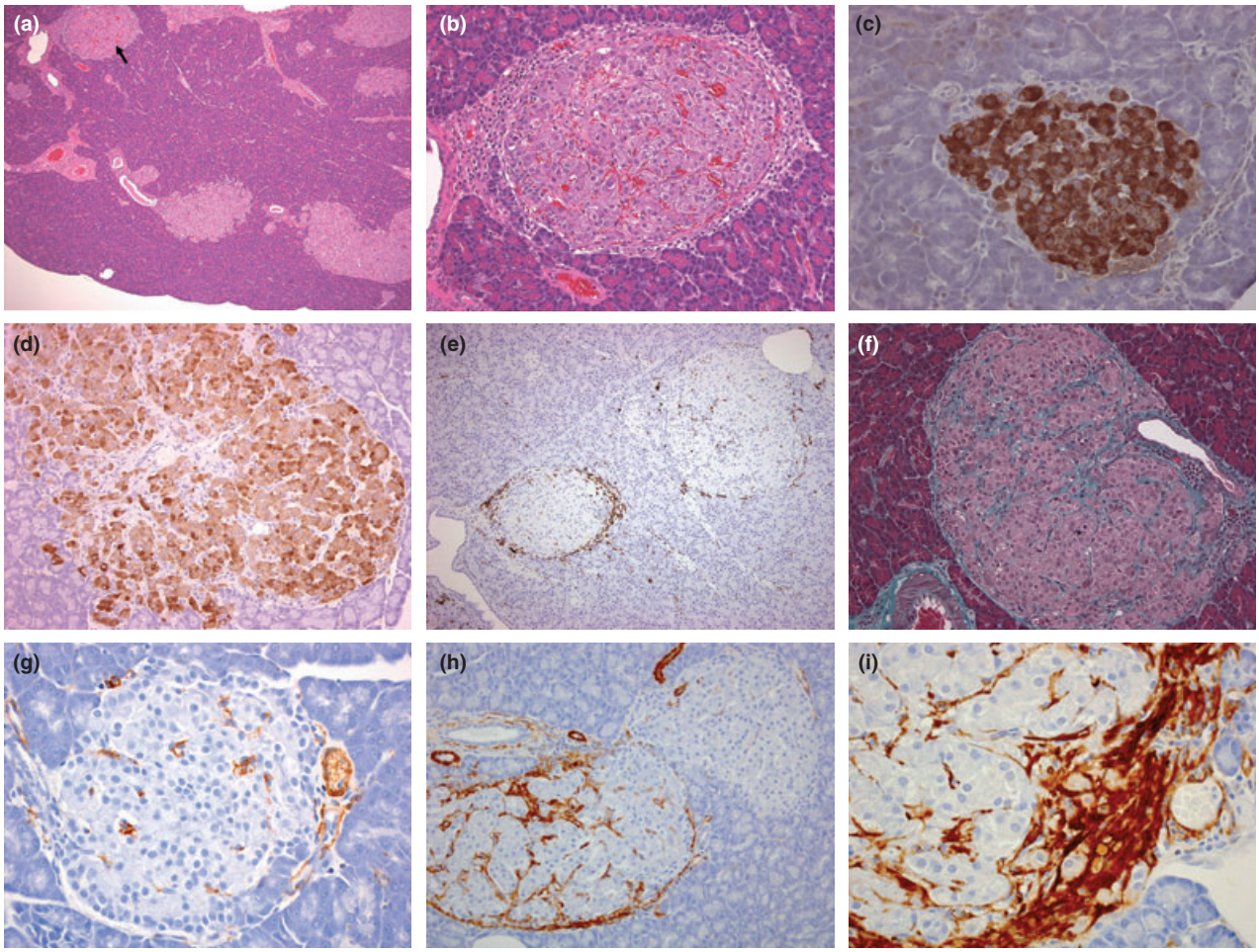

Figure 2 Islet characteristics of Zucker Fatty (ZF) rats. (a) 14 weeks, with multiple hyperplastic/hypertrophic islets, one of which (arrow) and at higher magnification, (b) illustrates the differences between islets in degree of mononuclear cell infiltration, vascular congestion/haemorrhage and fibrous tissue present (H&E), (c) 6 weeks, intense diffuse insulin staining compared with (d) 14 weeks, in this hypertrophic/hyperplastic islet, β cells are separated into groups by increased interstitial tissue and insulin staining is generally paler and more heterogeneous, (e) 14 weeks, two adjacent islets showing substantially different mononuclear infiltration, which in the smaller islet, is focussed principally around the periphery and illustrates the spectrum of islet changes in these animals (ED1), (f) 14 weeks, hypertrophic islet with increased fibrous tissue separating β cells into groups (Masson's Trichrome), (g) 6 weeks, sparse islet SMA staining; note vascular associated staining, (h) 14 weeks, two adjacent islets show different degrees of SMA staining associated with islet periphery, inter β cell perivascular tissue and in extra-islet periductal and vascular locations, (i) 14 weeks, islet periphery with active SMA-positive mesenchymal proliferation.

It is noteworthy that at 14 weeks, more islets showed lesions of substantially greater severity than those seen at 6 weeks or in obese ZFs. The predominant feature was that of considerable intra- and inter-animal variation in degrees of islet degeneration, with the hypertrophy/hyperplasia observed previously at 6 weeks being largely reduced. Additionally, apoptotic death was present more commonly, though at very low incidence. Occasionally, the extent of degeneration was such that β-cells were markedly reduced in numbers or appeared absent within the islet that now consisted of fibroblasts, fibrous connective tissue and very few ED1-positive mononuclear cells. In a few instances, fibrous scars were visible, indicative of lost islets. At this time, the irregular appearance of most islets was not associated with β-cell hypertrophy/hyperplasia, but was due to recruitment of mononuclear cells, substantially elevated numbers of fibroblasts and collagen deposition. Very few T (CD3) lymphocytes were present in islet-associated mononuclear cell infiltrates (Figure 3j), with typically only a few present in the entire pancreas section. No B (CD79a) lymphocytes were observed.

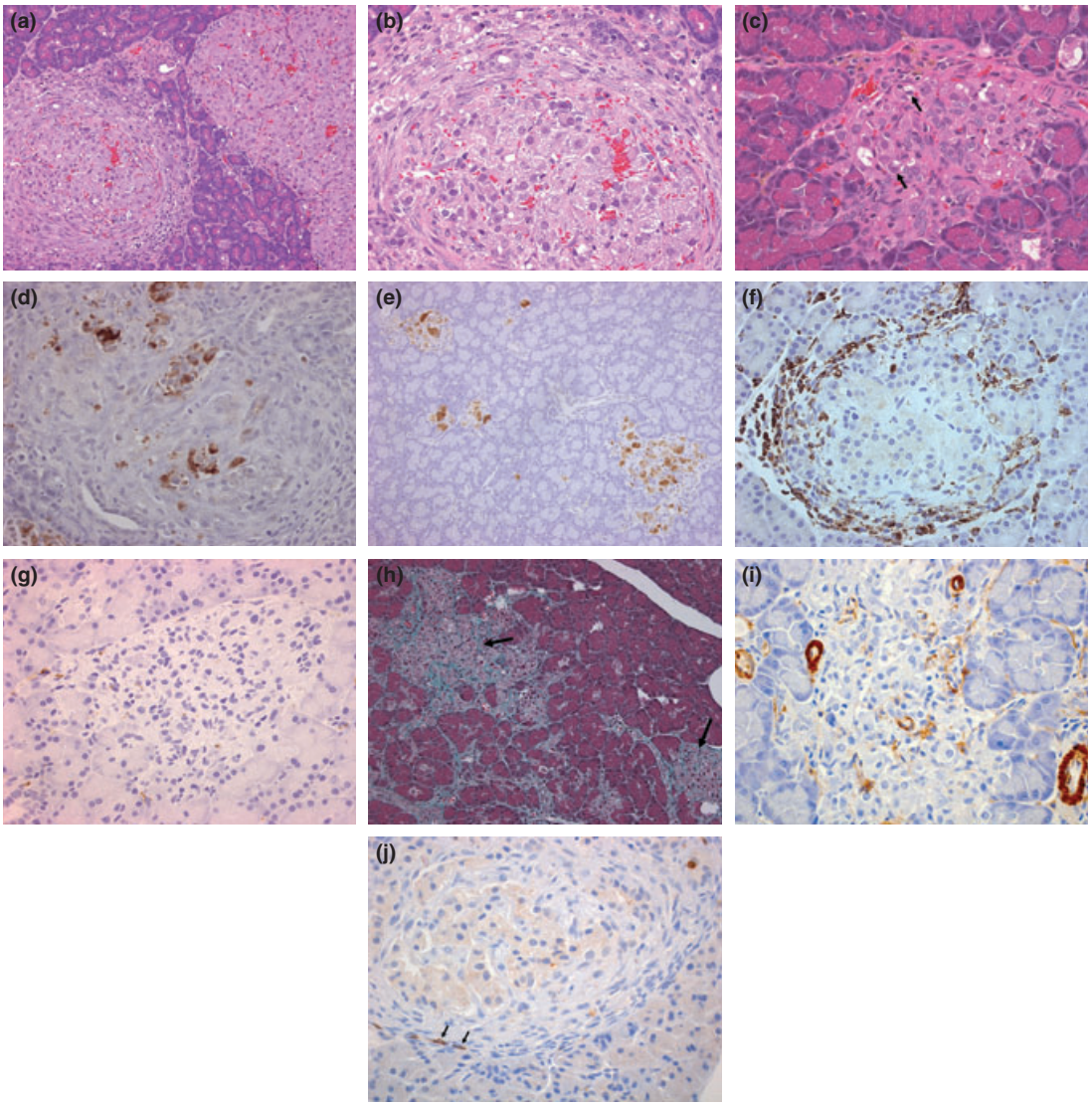

Figure 3 Islet characteristics of Zucker Diabetic Fatty (ZDF) rats. (a) 6 weeks, two islets showing substantially different appearances. On the right, this hypertrophic islet shows compression of adjacent exocrine tissue, vascular congestion/haemorrhage is prominent and peripheral endocrine cells are segregated into linear clusters. The left islet shows similar congestion/haemorrhage and β cells are vacuolated. The striking feature of this islet, that distinguishes it from its neighbour is the peri-islet layer of mononuclear cells and fibrous tissue, these being largely absent from the interior. Some β cell loss is also present as hyperchromatic cell debris. (Note that the changes observed in these islets are similar to those present in ZF islets, at 14 weeks, H&E), (b) 6 weeks, increased magnification of islet showing substantial, diffuse β cell vacuolation, β cell death inter-lacing, thin skeins of fibrous tissue and vascular congestion/haemorrhage (H&E), (c) 14 weeks, degenerate islet showing reduced β cell numbers, β cell vacuolation and degeneration (arrows) and numerous mesenchymal cells (H&E), (d) 6 weeks, substantial degeneration in this islet showing depleted numbers of β cells and heterogeneous insulin immunostaining, illustrating the rapidity of onset of degenerative changes in this strain, (e) 14 weeks, diffuse islet degeneration showing reduced and heterogeneous insulin staining in all islets, (f) 6 weeks, peri-islet monocyte/macrophage distribution illustrating the often substantial infiltration at this time (ED1), (g) 14 weeks, monocyte/macrophage infiltration almost absent in this severely degenerate islet which shows very few β cells, islet tissue replaced with fibrous tissue (ED1), (h) 14 weeks, abundant collagen distribution in two degenerate islets (arrows) and interconnecting in adjacent areas (Masson's Trichrome), (i) 14 weeks, severely degenerate islet showing little SMA immunopositivity of the islet, but present in islet pericytes and extra-islet vascular smooth muscle, (j) few T (CD3 positive) lymphocytes (arrows) in peri-islet fibroproliferative tissue.

Insulin immunostaining of neogenic clusters, small and large islets in 6 weeks old obese ZDF rats showed a heterogeneous pattern. At 14 weeks, β cells were substantially reduced in numbers (those remaining being widely separated by interstitial tissue) and displayed marked differences in staining intensity, very few being intensely brown whilst the majority were very lightly stained indicative of hyper-secretion. In obese ZDFs at 6 weeks, in the majority of islets, SMA-α immunostaining, was as seen in AP and Han Wistars, the remainder showing substantially increased inter β cellular staining of islet tissue. This SMA-α immunostaining of islet fibrous tissue seen at this time was absent at 14 weeks although all extra-islet tissue components (vascular, periductal) that normally stained positive for SMA were stained, representing a striking difference in islet condition between this strain and others. By comparison, Masson Trichrome-positive fibrous tissue staining in these older animals was markedly increased in both intra- and extra-islet tissue indicative of substantial collagen deposition.

β cell replication. β cell replication as shown by Ki67 expression showed an age-related reduction in all rat strains (Table 2). AP and HW rats showed 5.9× and 3.8× decreases respectively, with similar reductions seen in both lean and obese ZDF rats. Lean ZF rats showed the greatest reduction of approximately 13× from an initial level of 4% at 6 weeks to 0.29% at 14 weeks. Obese ZF rats maintained a high β cell replicative rate at 14 weeks, with an age-related reduction of 0.5× between 6 and 14 weeks as compared with AP rats of the same age.

β cell neogenic clusters. β cell neogenesis was significantly higher in all rat strains at 6 weeks by comparison with 14 weeks and highest in 6 weeks HW rats at 2.1/cm^2. All strains showed no significant difference from AP or HW rats at 6 weeks with the exception of obese ZDF rats (lower). At 14 weeks, lean ZF, lean ZDF and obese ZDF rats showed significantly lower β cell neogenesis than AP rats. This reduction was most marked in 14 weeks obese ZDF rats in which β cell neogenesis was less than 30% of other rat strains at this time and showed a 5.5× decrease at 14 weeks compared with the low value seen at 6 weeks.

Mean islet size. With the exception of obese ZF rats, no significant change in mean islet size was observed between 6 and 14 weeks in all rat strains. At 14 weeks, obese ZF rats showed a 2.5× increase in mean islet size and were approximately 1.5–2× larger than in the majority of other strains, with the exception of obese ZDF rats at this time, which were of similar dimensions.

Insulin-Positive Islet Area (IPIA). IPIA varied from 28 to 46% in all strains except obese ZDF rats at both time points. Obese ZDF rats showed a statistically significant and markedly lower IPIA at 6 and 14 weeks of 18% and 10% respectively by comparison with all other strains. No significant

Table 2 Islet parameters at 6 and 14 weeks

	6 weeks					
	AP	**HW**	**Lean ZF**	**Obese ZF**	**Lean ZDF**	**Obese ZDF**
β cell replication (%)	2.52 ± 0.43	1.8 ± 0.49	4.0 ± 0.55	2.9 ± 0.34†	1.5 ± 0.26 ‡	1.9 ± 0.32
Neogenic islet clusters (N/cm^2 pancreas)	1.7 ± 0.19	2.1 ± 0.20	1.1 ± 0.15	1.8 ± 0.24	1.1 ± 0.20	0.66 ± 0.10‡
Mean islet size (mm^2)	0.91 ± 0.08	0.98 ± 0.09	0.95 ± 0.27	0.76 ± 0.16	0.71 ± 0.12	1.71 ±0.29
Insulin positive islet area (%)	37 ± 1.6	41 ± 9.7	44 ± 2.0	44 ± 5.7	28 ± 7.1	18 ± 4.1‡
Islet β cell density (no./mm^2)	62 ± 3	72 ± 5	66 ± 5	64 ± 4	62 ± 3	38 ± 4 †‡
	14 weeks					
	AP	HW	Lean ZF	Obese ZF	Lean ZDF	Obese ZDF
β cell replication (%)	0.43 ± 0.11*‡	0.47 ± 0.08*	0.29 ± 0.10*‡	1.6 ± 0.47†	0.51 ± 0.14*‡	0.63 ± 0.22*
Neogenic islet clusters (N/cm^2 pancreas)	1.1 ± 0.04	0.87 ± 0.11*	0.68 ± 0.06*	0.99 ± 0.05*†	0.6 ± 0.04‡	0.12 ± 0.04*†‡
Mean islet size (mm^2)	1.21 ± 0.17 ‡	1.21 ± 0.19‡	1.14 ± 0.16‡	1.89 ± 0.18*†	1.06 ± 0.20	1.87 ± 0.34
Insulin positive islet area (%)	44 ± 2.2‡	34 ± 4.1	34 ± 1.3 *	32 ± 2.1	46 ± 2.1*‡	10 ± 0.7†‡
Islet β cell density (no./mm^2)	64 ± 3	67 ± 4‡	57 ± 3	47 ± 3*	61 ± 3	29 ± 1*‡

$^{*}P$ value of <0.05 *vs.* 6 weeks equivalent.
$^{\dagger}P$ value of <0.05 *vs.* lean equivalent.
$^{\ddagger}P$ value of <0.05 *vs.* obese ZF.

increase in IPIA was observed in any strain between 6 and 14 weeks. Lean ZF rats showed a slight age-related reduction in IPIA from 44% at 6 weeks to 34% at 14 weeks.

Islet β cell density. There were approximately 62–72 β cells/mm^2 (mean values) in all rat strains at 6 weeks with the exception of obese ZDF rats, which showed a substantial reduction in islet β cell density of almost half that in other strains (38/mm^2). In obese ZDFs, significant further reductions were observed at 14 weeks when β cell density was decreased to 29/mm^2. A statistically significant decrease in β cell density was also observed in obese ZF rats at 14 weeks compared with the 6 weeks value. Furthermore, β cell density was decreased slightly at 14 weeks in obese ZF rats compared with HW rats at this time.

Discussion

This study focussed on the plasma biochemical and morphological characteristics of islets of Langerhans in 6 or 14 weeks old diabetic and non-diabetic strains of rat, maintained on standard diet. These ages were selected as they represent pre-diabetic and diabetic conditions in the obese ZDF rat (Peterson *et al.* 1990). No significant morphological differences were observed in AP, HW, lean ZF and lean ZDF animals at either timepoint. However, the lean ZF and ZDFs displayed minor changes in some plasma chemistry parameters at both timepoints namely, lowered plasma insulin and triglycerides. Lean ZFs showed lowered free fatty acids, although in lean ZDFs these were normal or mildly increased. Hypoinsulinaemia in these animals may be directly related to low plasma triglycerides and/or free fatty acids and explained by control of or, reduction in lipotoxic influences on β-cells (Unger 2002). Indeed, evidence in support of this notion is provided by reduction of hyperlipacidaemia and hyperlipidaemia through controlling hyperphagia of obese ZDFs: pair feeding with lean littermates reduced all β-cell abnormalities and prevented hyperglycaemia. (Ohneda *et al.* 1995).

Obese ZFs at 6 weeks were euglycaemic and showed only a minor increase in plasma insulin with no changes in islet morphology or insulin immunostaining pattern. Islet parameters in general, were not significantly altered from other strains. By comparison, at 14 weeks, these animals remained euglycaemic, had become markedly hyperinsulinaemic and morphologically, showed several islet appearances, principally of hypertrophy/hyperplasia, whilst a minority of islets were degenerative. The increased level of insulin resistance in this strain is regarded as the stimulus for these adaptive (hypertrophic/hyperplastic) islet changes to maintain glucose homeostasis and euglycaemia (Bonner-Weir 2001) and represents a valid model of islet adaptation in human insulin resistance and associated hyperglycaemia. Given the biochemical evidence, the heterogeneous islet morphologies present are an interesting feature, as clearly, all islets do not respond in the same way and at the same time to blood-borne, chemical messengers of systemic tissue glucose utilisation. In these animals, the physiological outcome of euglycaemia is constructed upon a base of marked hyperinsulinaemia (approximately 8–11× HW or AP) due to β-cell hypertrophy/hyperplasia. The key features of the majority of islets at this time was the substantial elevation in Ki67-assessed β-cell replication which was several fold that in AP, HW and lean ZFs, in conjunction with reduced islet β-cell density, reduced IPIA and mildly increased mean islet size. In our study, no markers of β-cell apoptosis were employed to evaluate the balance between recruitment to and loss from this population due to the relatively few β-cells present in tissue sections, but it is clear that the other measures employed support a view of substantially increased β-cell turnover (Bonner-Weir 2001).

Obese ZDFs displayed moderate hyperinsulinaemia and euglycaemia at 6 weeks but at 14 weeks this profile had reversed such that the animals were hyperglycaemic and slightly hypoinsulinaemic by comparison with HW or AP rats. The morphology of the majority of islets in these animals at 6 weeks reflects the plasma chemistry profiles, as islets were generally hypertrophic with a small minority only, showing combined hypertrophy and degenerative changes and which would appear to account for the moderate hyperinsulinaemia observed. Whilst, β-cell replication was similar to that in HW or APs, mean islet size was about double that of non-diabetic rat islets and IPIA and islet β-cell density were substantially reduced, being approximately 50% of values in these other strains. This evident disparity is accounted for by increased and variable islet inflammatory cell infiltration and fibrosis. Neogenic β-cell clusters were substantially reduced by comparison with non-diabetic controls. At 14 weeks, islet degeneration had progressed to such a degree that insufficient insulin was generated by the remaining β-cells as demonstrated by immunohistochemistry and consequently, hyperglycaemia was substantial in these animals (32.5 mM, approximately four fold greater than APs). β-cell replication was substantially reduced by comparison with obese ZDFs at 6 weeks and similar to that in non-diabetic controls at 14 weeks. Whilst mean islet size remained significantly increased by comparison with non-diabetic controls, IPIA, islet β-cell density and the incidence of neogenic β-cell clusters were all substantially reduced. In contrast, islet fibrosis, as indicated by Masson Trichrome staining was often substantial.

Our observations of increased β-cell degeneration and death in obese ZDFs and obese ZFs with reduction both in insulin immunostaining and in viable islet tissue accord with those of several investigators (Pick *et al.* 1998; Janssen *et al.* 2001, 2003). However, by comparison with studies such as those of Pick *et al.* (1998), four important differences between non-diabetic control rats and obese ZFs and ZDFs are notable in the present study, although the latter strain exhibit these changes earlier and to a greater severity. Firstly, substantial islet morphological heterogeneity, secondly, increased vascular dilatation and congestion with recent haemorrhage and occasionally, some pigment in obese ZDFs, thirdly, the often substantial infiltration of mainly ED1-positive mononuclear cells (with some T lymphocytes) into and around islets, fourthly, elevated fibrosis seen in a minority of islets often associated with and following peri-islet mononuclear cell infiltration and distinct from the reticular pattern of fibrosis that accompanies neovascularisation during adaptive hypertrophy/hyperplasia.

Islet vascular changes were present only in obese animals, were most prominent in obese ZDFs and showed substantial intra- and inter-animal variation. Three spontaneously diabetic rat strains namely Goto-Kakisaki (GK), Spontaneously Diabetic Torii and Otsuka Long-Evans Tokushima fatty (OLETF) rats also display vascular and blood flow alterations during development of the disease (Atef *et al.* 1992, 1994; Carlsson *et al.* 1997; Mizuno *et al.* 1999; Iwase *et al.* 2002; Masuyama *et al.* 2004; Svensson *et al.* 2006; Homo-Delarche *et al.* 2006). Jansson and Hellerstrom (1986) demonstrated that intra-carotid infusion of glucose into adult Sprague-Dawley rats, induced rapid increase in plasma insulin and islet blood flow (without any alteration in pancreatic blood flow) and concluded that islet insulin release was mediated via systemic glucose concentrations whilst islet blood flow was controlled via plasma glucose-induced vagal cholinergic stimulation. Atef *et al.* (1992) showed that obese, hyperglycaemic rats have a higher islet blood flow and are hyperinsulinaemic by comparison with their lean counterparts and implicated both parasympathetic and sympathetic influences in this control. The regulation of islet blood flow is complex and depends upon balanced vasoconstriction and vasodilatation involving numerous factors. NO is a potent endothelium-derived vasodilating agent generated in noradrenergic, non-cholinergic nerves terminating on vascular smooth muscle cells. NO generation is catalysed by nitric oxide synthase (constitutively expressed in peripheral nerves, the CNS and endothelial cells and inducible in many cell types including islet cells and inflammatory cells) and its islet vasodilating effects are reversed by inhibition of NO synthase through N^G-nitro-L-arginine (Svensson *et al.* 2006). It is plausible therefore that the vascular changes seen in our study are related, at least in part, to sustained hyperglycaemia and hyperlipacidaemia. Indeed, Shimabukuro *et al.* (1997) demonstrated that FFA-induced suppression of insulin release in prediabetic ZDF islets in vitro was characterised by substantial NO release by comparison with controls and associated with upregulated iNOS mRNA. These changes are effectively reversed by nicotinamide and aminoguanidine, potent NO-lowering agents, as their administration to prediabetic ZDF rats prevents islet iNOS expression, decreased β-cell dysfunction and blocked β-cell destruction and hyperglycaemia. Endothelial functional perturbation is a characteristic feature of diabetes and responsible for significant pathologies in different systems. Hyperglycaemia activates islet endothelial cells and induces generation of islet proinflammatory cytokines resulting in recruitment of leucocytes (Morigi *et al.* 1998; Booth *et al.* 2001; Takaishi *et al.* 2003). Exacerbation of these inflammatory events occurs by activated macrophage release of extra cellular matrix-related molecules, inflammatory cytokines, growth factors and chemokines (Shanmugam *et al.* 2003; Devaraj *et al.* 2005; Donath *et al.* 2008).

Common to both ZF and ZDF rats was the key morphological feature of islet degeneration namely, mononuclear cell infiltration that either preceded or coincided with fibroproliferation leading to mature fibrous tissue and was significantly more prominent in the latter strain. Notably, this inflammatory cell infiltration is free of polymorphonuclear neutrophils in any islet examined, regardless of condition, distinguishing it clearly from an acute inflammatory response to a necrotic stimulus. However, it does occasionally contain a very small number of T lymphocytes suggestive of an inflammatory and not an autoimmune response. The fibroproliferation observed was different from that seen during islet adaptation by β cell hypertrophy/hyperplasia, in which sparse fibrous tracts associated with neovascularisation, separated β-cells into groups. Initially, almost pure populations of mononuclear inflammatory cells pervaded the islet margin and often lay between adjacent exocrine tissue and the outermost layers of islet tissue. These ED1-positive cells constituted a population of monocytes that in some instances appeared in association with a vigorous proliferation of mixed SMA-α-positive mesenchymal cells that may include macrophages, smooth muscle cells, pericytes and myofibroblasts (Gabbiani 2003; Hinz *et al.* 2007). The variation between islets in their display of ED1-positive mononuclear cells and fibroproliferation was substantial. Manifestly, all islets were dissimilar in this regard; adjacent islets often showing substantial variation in inflammatory cell association and both adaptive and reactive

fibroproliferation. The spectrum of islet degeneration that initially displayed mononuclear cell infiltration with fibroproliferation and fibrosis, with sequential loss of markers of these processes, culminated in fibrotic islet remnants (scars). Numerous elements of this pattern of islet failure have also been seen in another diabetic rat strain, the GK rat (Homo-Delarche *et al.* 2006). These workers compared non-diabetic Wistar and GK rats at 1, 2 and 4 months using histological, immunohistochemical and gene expression analysis with Affymetrix microarrays and found no significant histological alterations in islets of 1-month-old Wistar or GK rats. However, at 2 months (after 1 month of mild hyperglycaemia) considerable increases were noted, most significantly in infiltration of macrophages, degree of fibrosis and extent of vascularization. These findings accord with those of our study of obese rat islets in which increased vascularization/fibrosis between intra-islet β-cell clusters occurred in obese ZF and ZDF rats during islet hypertrophic adaptation in physiological conditions of mild hyperglycaemia, islet fibrosis progressing during the duration of hyperglycaemia. Moreover, of 71 genes found to be over-expressed in 4-month-old GK rat islets, 24% and 34% respectively belonged to extra cellular matrix /cell adhesion and inflammatory/immune response families. In a synthesis of the morphological and genetic events occurring in the GK rat during islet failure, Homo-Delarche *et al.* (2006) suggested that the primary events are likely to occur in the intra- and peri-islet vascular endothelial and smooth muscle cells in their secretion of cytokine production and adhesion molecule expression leading to attraction and migration of inflammatory cells (Morigi *et al.* 1998; Booth *et al.* 2001; Takaishi *et al.* 2003). Activated macrophages generate chemokines, extracellular matrix molecules, proinflammatory cytokines and growth factors (Nathan 1987; Homo-Delarche & Drexhage 2004). Furthermore, hyperglycaemia stimulates monocyte/macrophage secretion of numerous proinflammatory factors such as interleukins (IL)-1 and -6, tumour necrosis factor α and transforming growth factor β1. In this context, neutralisation of the proinflammatory effects of IL1-β by antibody administration in hyperglycaemic, diet induced obese mice (Osborn *et al.* 2008) and an IL1-β antagonist in type II diabetic patients (Larsen *et al.* 2007) resulted in improved glycaemic control and β-cell function with lowered circulating inflammatory markers. These stimuli and proinflammatory influences on cell recruitment and function and their direct relationship to glycaemia differentiate the diabetic from the non-diabetic rat strains assessed in our study. These findings in this rat strain are resonant of recent work that has demonstrated the presence of CD68+ macrophages in the islets of human NIDDM patients (Ehses *et al.* 2007; Richardson *et al.* 2009). These workers demonstrated that although few macrophages were present in the islets of NIDDM patients, significantly greater numbers were seen by comparison with non-diabetic age-matched controls. Hyperglycaemia-induced IL1-β secretion by human β-cells occurring prior to leucocyte infiltration and substantial β-cell death and later, fibrosis, pathognemonic of late stage chronic inflammation has been described by Donath *et al.* (2008, 2009) and Ehses *et al.* (2009) and brings into sharp focus the importance of islet inflammation in human diabetes. The numerous intra- and extra-islet processes relating to cause and effect of human islet inflammatory processes in NIDDM are reflected by similar changes in islets of obese ZDF rats and other obese rodents and may offer investigative opportunities in their dissection.

The focus of this report has been the stark differences in islet characteristics of non-diabetic and diabetic Wistar-derived rat strains. We have demonstrated substantial vascular and inflammatory changes in islets of insulin resistant and diabetic strains that are absent in non-diabetic strains. However, the primary feature(s) that confers upon certain islets a predisposition to inflammatory cell ingress and consequent further degeneration and fibrosis remains unknown. This characteristic of these islets in diabetic strains of rat may offer insight into the pathogenesis of NIDDM. Whether or not endothelial cell or islet blood flow perturbations, β-cell or endothelial cell inflammatory mediator secretion, extracellular matrix glycation products (Brownlee 1995; Wautier & Guillausseau 2001), islet β-cell functional integrity/activity or other influences are primarily involved in individual islet susceptibility is an important issue.

Acknowledgements

We are obliged to the staff of the Diabetes, Histology, Clinical Pathology and Analytical Morphology groups at AstraZeneca, Alderley Park for their expert contributions to this work and to Drs Anna Marley, David Smith, Julie Chambers and Johannes Harleman for valuable discussions.

References

Atef N., Ktorza A., Picon L., Penicaud L. (1992) Increased islet blood flow in obese rats: role of the autonomic nervous system. *Am. J. Physiol.* **262**, E736–E740.

Atef N., Portha B., Penicaud L. (1994) Changes in islet blood flow in rats with NIDDM. *Diabetologia* **37**, 677–680.

Bonner-Weir S., (2001) β-Cell turnover. Its assessment and implications. *Diabetes* **50**, S20–24.

Booth G., Stalker T.J., Lefer A.M., Scalia R. (2001) Elevated ambient glucose induces acute inflammatory events in the microvasculature: effects of insulin. *Am. J. Physiol. Endocrinol. Metab.* **280**, E848–E856.

Brownlee M. (1995) Advanced protein glycosylation in diabetes and aging. *Annu. Rev. Med.* **46**, 223–234.

Carlsson P.O., Jansson L., Ostenson C.G., Kallskog O. (1997) Islet capillary blood pressure increase mediated by hyperglycaemia in NIDDM GK rats. *Diabetes* **46**, 947–952.

Clark J.B., Palmer C.J., Shaw W.N. (1983) The diabetic Zucker Fatty rat. *Proc. Soc. Exp. Biol. Med.* **173**, 68–75.

Clark A., Wells C.A., Buley I.D. *et al.* (1988) Islet amyloid, increased A-cells, reduced B-cells and exocrine fibrosis: quantitative changes in the pancreas in type 2 diabetes. *Diabetes Res.* **9**, 151–159.

Devaraj S., Venugopal S.K., Singh U., Jialal I. (2005) Hyperglycaemia induces monocytic release of interleukin-6 via induction of protein kinase c-α and -β. *Diabetes* **54**, 85–91.

Donath M., Schumann D.M., Faulenbach M., Ellingsgaard H., Perren A, Ehses J.A. (2008) Islet inflammation in type 2 diabetes. *Diabetes Care* **31**, S161–S164.

Donath M.Y., Boni-Schnetzler M., Ellingsgaard H., Ehses J.A (2009) Islet inflammation impairs the pancreatic β cell in type 2 diabetes. *Physiology* **24**, 325–331.

Ehses J.A., Perren A., Eppler E. *et al.* (2007) Increased number of islet associated macrophages in type 2 diabetes. *Diabetes* **56**, 2356–2370.

Ehses J.A., Ellingsgaard H., Boni-Schnetzler M., Donath M.Y. (2009) Pancreatic islet inflammation in type 2 diabetes: from α and β cell compensation to dysfunction. *Arch. Physiol. Biochem.* **115**, 240–247.

Gabbiani G. (2003) The myofibroblast in wound healing and fibrocontractive diseases. *J. Pathol.* **200**, 500–503.

Hinz B., Phan S.H., Thannickal V.J., Galli A., Bochaton-Piallat M.L., Gabbiani G. (2007) The myofibroblast: one function, multiple origins. *Am. J. Pathol.* **170**, 1807–1816.

Homo-Delarche F. & Drexhage H.A. (2004) Immune cells, pancreas development, regeneration and Type 1 diabetes. *Trends Immunol.* **25**, 222–229.

Homo-Delarche F., Calderari S., Irminger J.-C. *et al.* (2006) Islet inflammation and fibrosis in a spontaneous model of type 2 diabetes, the GK rat. *Diabetes* **55**, 1625–1633.

Iwase M., Uchizono Y., Tashiro K., Goto D., Iida M. (2002) Islet hyperfusion during prediabetic phase in OLETF rats, a model of type 2 diabetes. *Diabetes* **51**, 2530–2535.

Janssen S.W.J., Martens G.J.M., Sweep C.G.J.F., Ross H.A., Hermus A.R.M.M. (1999) In Zucker Diabetic Fatty rats plasma leptin levels are correlated with plasma insulin levels rather than with body weight. *Horm. Metab. Res.* **31**, 610–615.

Janssen S.W.J., Hermus A.R.M.M., Lange W.P.H. *et al.* (2001) Progressive histopathological changes in pancreatic islets of Zucker Diabetic Fatty rats. *Endocrinol. Diab.* **109**, 273–282.

Janssen S.W.J., Martens G.J.M., Sweep C.G.J., Span P.N., Verhofstad A.A.J., Hermus A.R.M.M. (2003) Phlorizin treatment prevents the decrease in plasma insulin levels but not the progressive histopathological changes in the pancreatic islets during aging of Zucker diabetic fatty rats. *J. Endocrinol. Invest.* **26**, 508–515.

Jansson L. & Hellerstrom C. (1986) Glucose-induced changes in pancreatic islet blood flow mediated by central nervous system. *Am. J. Physiol. Endocrinol. Metab.* **14**, E644–E647.

Kloppel G., Lohr M., Habich K., Oberholzer M., Heitz P.U. (1985) Islet pathology and the pathogenesis of type 1 and type 2 diabetes mellitus revisited. *Surv. Synth. Pathol. Res.* **4**, 110–125.

Larsen C.M., Faulenbach M., Vaag A. *et al.* (2007) Interleukin-1-receptor antagonist in type 2 diabetes. *New Engl. J. Med.* **356**, 1517–1526.

Listenberger L.L., Xianlin H., Lewis S.E. *et al.* (2003) Triglyceride accumulation protects against fatty acid-induced lipotoxicity. *Proc. Natl Acad. Sci. USA* **100**, 3077–3082.

Masuyama T., Komeda K., Hara A. *et al.* (2004) Chronological characterisation of diabetes development in male Spontaneously Diabetic Torii rats. *Biochem. Biophys. Res. Commun.* **314**, 870–877.

Mizuno A., Noma Y., Kumajima M, Murakami T., Zhu M., Shima K. (1999) Changes in islet capillary angioarchitecture coincide with impaired β cell function but not with insulin resistance in male Otsuka-Long-Evans-Tokushima fatty rats: dimorphism of the diabetic phenotype at an advanced age. *Metabolism* **48**, 477–483.

Morigi M., Angioletti S., Imberti B. *et al.* (1998) Leucocyte-endothelial interaction is augmented by high glucose concentrations and hyperglycaemia in a NF-kβ-dependent fashion. *J. Clin. Invest.* **101**, 1905–1915.

Nathan C.F. (1987) Secretory products of macrophages. *J. Clin. Invest.* **79**, 319–326.

Ohneda M., Inman L.R., Unger R.H. (1995) Caloric restriction in obese pre-diabetic rats prevents beta-cell depletion, loss of beta-cell GLUT 2 and glucose incompetence. *Diabetologia* **38**, 173–179.

Osborn O., Brownell S.E., Sanchez-Alavez M., Salomon D., Gram H., Bartfai T. (2008) Treatment with an interleukin 1 beta antibody improves glycaemic control in diet induced obesity. *Cytokine* **44**, 141–148.

Paris M., Bernard Kargar C., Berthault M.F., Bouwens L., Ktorza A. (2003) Specific and combined effects of insulin and glucose on functional pancreatic β cell mass in vivo in adult rats. *Endocrinology* **144**, 2717–2727.

Pearse A.G.E. (1985) *Histochemistry. Vol 2. Analytical Technology*. Churchill Livingstone, Edinburgh, UK, P. 549.

Peterson R.G., Shaw W.N., Neel M.A., Little L.A., Eichenberg J. (1990) Zucker diabetic fatty rat as a model of non-insulin dependent diabetes mellitus. *ILAR J.* **32**, 16–19.

Pick A., Clark J., Kubstrup C. *et al.* (1998) Role of apoptosis in failure of β cell mass compensation for insulin resistance and β cell defects in the male Zucker diabetic fatty rat. *Diabetes* **47**, 358–364.

Poitout V. & Robertson R.P. (2008) Glucolipotoxicity: fuel excess and β cell dysfunction. *Endocr. Rev.* **29**, 351–366.

Rahier J., Goebbles R.M., Henquin J.C. (1983) Cellular composition of the human diabetic pancreas. *Diabetologia* **24**, 366–371.

Richardson S.J., Willcox A., Bone A.J., Foulis A.K., Morgan N.G. (2009) Islet-associated macrophages in type 2 diabetes. *Diabetologia* **52**, 1686–1688.

Rosenberg L. (1995) In vivo cell transformation: neogenesis of beta cells from pancreatic ductal cells. *Cell Tranplantation* **4**, 371–383.

Shanmugam M., Reddy M.A., Guha M., Natarajan R. (2003) High glucose-induced expression of proinflammatory cytokine and chemokine genesin monocytic cells. *Diabetes* **52**, 1256–1264.

Shimabukuro M., Ohneda M., Lee Y., Unger R. (1997) Role of nitric oxide in obesity-induced β cell disease. *J. Clin. Invest.* **100**, 290–295.

Shimabukuro M., Zhou Y.T., Levi M., Unger R.H. (1998) Fatty acid-induced β cell apoptosis: a link between obesity and diabetes. *Proc. Natl Acad. Sci. USA* **95**, 2498–2502.

Stefan Y., Orci L., Malaisse-Lagae F., Perrelet A., Patel Y., Unger R.H. (1982) Quantitation of endocrine cell content in the pancreas of nondiabetic and diabetic humans. *Diabetes* **31**, 694–700.

Svensson A.M., Ostenson C.-G., Sandler S., Efendic S., Jansson L. (2006) Inhibition of nitric oxide synthase by N^G-nitro-L-arginine causes a preferential decrease in pancreatic islet blood flow in normal rats and spontaneously diabetic GK rats. *Endocrinology* **135**, 849–853.

Takaishi H., Taniguchi T., Takahashi A., Ishikawa Y., Yokoyama M. (2003) High glucose accelerates MCP-1 production via p38 MAPK in vascular endothelial cells. *Biochem. Biophys. Res. Commun.* **305**, 122–128.

Tokuyama Y., Sturis J., DePaoli A.M. *et al.* (1995) Evolution of β cell dysfunction in the male Zucker Diabetic Fatty rat. *Diabetes* **44**, 1447–1457.

Unger R.H. (2002) Lipotoxic diseases. *Annu. Rev. Med.* **53**, 319–336.

Wautier J.L., Guillausseau P.J. (2001) Advanced glycation end products, their receptors and diabetic angiopathy. *Diabetes Metab. (Paris)* **27**, 535–542.

Zhou Y.-T., Grayburn P., Karim A. *et al.* (2000) Lipotoxic heart disease in obese rats: implications for human obesity. *Proc. Natl Acad. Sci. USA* **97**, 1784–1789.

